

# Construct a stable super-hydrophobic surface through acetonitrile extracted lignin and nano-silica and its application in oil-water separation

Xiaoyu Gong, Yi Meng, Junjie Zhu, Xing Wang, Jie Lu, Yi Cheng, Yehan Tao\*, Haisong Wang\*

Liaoning Key Laboratory of Lignocellulose Chemistry and BioMaterials, Dalian Polytechnic University, Dalian, 116034, Liaoning, China



## ARTICLE INFO

### Keywords:

Acetonitrile extracting lignin  
Superhydrophobic filter paper  
Oil/water separation

## ABSTRACT

It remains a great challenge for the simple, environmentally friendly and low-cost production of oil/water separation membrane. Under this backdrop, a highly efficient membrane based on filter paper, acetonitrile extracting lignin and silica is reported. Two impregnation steps are involved for the membrane preparation, firstly, a thin layer of lignin is coated on the surface of the filter paper and then, silica nanoparticles are adhered to the pre-coated filter paper, leading to the formation of a micro-nano binary structure, which turns the hydrophilicity nature of the filter paper into lipophilicity and strong hydrophobicity. The modified filter paper has a contact angle of 168°, which is 118° higher than that of a reference membrane prepared by technical lignin and silica nanoparticles. The modified filter paper exhibits an excellent separation efficiency as high as 98.6% in the process of oil/water separation. Notably, considering the applied low-cost substrates and the simple dipping operation, this modification route is expected to be easily extended to a versatile of other substrates that need to be hydrophobized.

## 1. Introduction

Oil-water separation process has drawn great attention considering (Feng et al., 2004; Yan et al., 2020), controlling the serious contamination of oily wastewater produces from various industries, and the importance of purifying fuel oil from the economic point of view (Cheryan and Rajagopalan, 1998). The water resistant(Hu et al., 2009) and self-cleaning(Chen et al., 2018) properties of the superhydrophobic material, together with its special wetting properties(Wang et al., 2010; Zhu et al., 2011), make it very lipophilic and can be applied for the separation of attached oil-water mixtures(Zhang et al., 2020). In recent years, different methods have been applied for endowing superhydrophobicity to a variety of substrates, for example, Li et al.(Li et al., 2007) prepared a superhydrophobic surface with a petal-like structure on a nickel metal substrate by a simple chemical method using mono-alkyl phosphoric acid. Zhang et al.(Zhang et al., 2020) modified carbon nanofibers on polyurethane nanofibers, and then modified poly-dimethylsiloxane to prepare flexible, stretchable, super-hydrophobic/super-hydrophobic nanofiber composite membrane. Even though these superhydrophobic materials have achieved good separation performance(Lu et al., 2020), their substrates have many limitations, such as high-cost, environmentally unfriendly, poor

operability, and narrow application range(Liu et al., 2013; Ma et al., 2005; Xu et al., 2011).

On the other hand, lignin, as the second most abundant plant polymer on earth and the only non-petroleum resource that can provide renewable aromatic compounds in nature(Chio et al., 2019; Meng et al., 2020; Wen et al., 2013), and most importantly, possessing strong hydrophobicity, is a quite cheap and environmentally friendly candidate for preparing superhydrophobic material(Xia et al., 2020). However, the efficient utilization of lignin is still difficult to access. According to incomplete statistics, only 5% of technical lignin can be converted to high value-added products such as additives(Klapiszewski et al., 2020), dispersants(Peng et al., 2020), adhesives(Gong et al., 2020; Raj et al., 2020; Venkatesagowda and Dekker, 2019) and surfactants(Chen et al., 2019). It can be seen that the current lignin processing methods have caused a huge waste of bio-based resources and brought increasingly environmental pollution problem. Recently, there are literatures of lignin-based samples for oil/water separation: A lignin-based carbon aerogel enhanced by graphene oxide was fabricated (Meng et al., 2020). The synergistic effect of superhydrophobicity and good mechanical property acquired by lignin derivate and graphene oxide ensures the carbon aerogel appropriate for oil/water separation and light oil, heavy oil and emulsified oil are separated respectively by the gel. A

\* Corresponding authors.

E-mail addresses: [taoyh1818@dlpu.edu.cn](mailto:taoyh1818@dlpu.edu.cn) (Y. Tao), [wanghs@dlpu.edu.cn](mailto:wanghs@dlpu.edu.cn) (H. Wang).



**Fig. 1.** The preparation process and mechanism diagram of paper composite materials.

lignin-modified membrane was prepared via layer-by-layer assembly that also obtains an oil/water separation sample (Shamaei et al., 2020). a suspension of lignin and beeswax was coated on cotton to form a low surface energy sample that applied for oil/water separation (Zhang et al., 2019). Therefore, better utilization of lignin, such as applying lignin in superhydrophobic paper-based composites for oil-water separation that uses lignin's own hydrophobic and lipophilic properties has drawn growing research interest.

Superhydrophobic paper-based composites can be prepared by applying surface impregnation (Wang et al., 2010), coating (Fu et al., 2019) and fiber modification (Roy et al., 2009) to paper matrix. Filter paper, one of the paper matrix composite materials, can separate useless substances or impurities from gas or liquid in order to recycle useful substances. In recent years, superhydrophobic preparation method has been used in filter paper, which gives filter paper many special functions, such as oil-water separation when the surface of filter paper has a special wetness (Tang et al., 2017). Wang et al. (2017) reported that hydrophobic titanium dioxide nanoparticles were dispersed into carnauba wax-ethanol emulsion to form a composite coating on filter paper, leading a good hydrophobicity and stability against acid or alkali solution. After fully dispersing the polystyrene in toluene reagent, Wang et al. (Wang et al., 2010) added a certain amount of hydrophobic silicon dioxide nanoparticles into the mixture and soaked the filter paper with mixed solution. The as-prepared filter paper was hydrophobic and can absorb diesel oil drifting on the water or emulsified oil in water. Kong et al. (Kong et al., 2014) prepared low-cost and highly efficient paper-based membranes for oil/water separation through only two steps: a thin layer of aluminum oxide was primary covered on the surface of the filter paper by nuclear layer deposition, and silane particles needed aid therefore coupled on the precoated aluminum oxide layer through their response for hydroxyl aggregations on the surface. Current preparation routes of superhydrophobic paper-based composites still display some drawbacks, ranging from requiring multistep, strict preparation environment and instruments, and some not environmentally friendly or even expensive ingredients.

Under this background, it is of great importance to developing a simple, environmental-friendly and economical method to prepare efficient paper-based composites. In this work, we incorporated the acetonitrile extracted lignin (AEL) with high purity, more phenolic hydroxyl groups, carboxyl groups and narrow molecular weight dispersity, which can improve the bonding strength with filter paper, was incorporate with silica nanoparticles to form a stable micro nano binary structure as a super hydrophobic surface for oil-water separation. This simple and low-cost superhydrophobic preparation opens up a new route for the efficient utilization of lignin and in perspective, this kind of

economical route for constructing an efficient and stable superhydrophobic surface provides a new idea for preparing oil/water separation materials.

## 2. Materials and methods

### 2.1. Materials

The paper selected in the experiment is ordinary medium speed qualitative filter paper (FP) ( $\Phi = 9$  cm in diameter), purchased from Hangzhou special paper industry Co., Ltd. (Zhejiang, China). Technical lignin (TL) was provided by Yueyang Forest & Paper Co. Ltd. (Yueyang, Hunan China). Acetonitrile (AR) was purchased from Kermel Reagent Co., Ltd. (Tianjin, China). Ethyl alcohol (AR) was purchased from DaMao Reagent Co., Ltd. (Tianjin, China). Hydrophobic Silicon dioxide (> 99% metals basis) was provided by Macklin Reagent. Light petroleum (AR, 60–90) was purchased from Xinxing Reagent Co. Ltd. (Liaoning, China). Unless otherwise specified, all reagents are used in accordance with accepted standard.

### 2.2. Experiments

#### 2.2.1. Preparation of acetonitrile extracted lignin (AEL)

AEL used in this study was extracted from technical lignin (TL) by acetonitrile, as a reported method (Cui et al., 2018). 50 g of as-received lignin was stirred in 500 mL of acetonitrile, and then the mixture was centrifuged to separate insoluble part. The solvent was removed and recollected by a rotary evaporator, and then the product, AEL, was obtained.

#### 2.2.2. Preparation of impregnation liquid of paper composite

2 g AEL was added in 18 g ethanol, fully dissolved and centrifuged, then took the supernatant and marked it as solution 1. Adding 0.2 g silica nanoparticles to 20 g petroleum ether solvent and dispersed uniformly as solution 2.

#### 2.2.3. Preparation of superhydrophobic paper matrix composites

Dipping the filter paper in the two solutions orderly is shown in Fig. 1. The impregnation time of the paper base in the first solution was 5 min, and that in solution 2 was 20 min. After the paper was impregnated, it was dried in an oven at 80 °C for 10 min. The prepared AEL-based paper composite (AEL-FP) was weighed with an analytical balance. The control group TL-based filter paper composite (TL-FP) was prepared in the same method except for using TL instead of AEL.

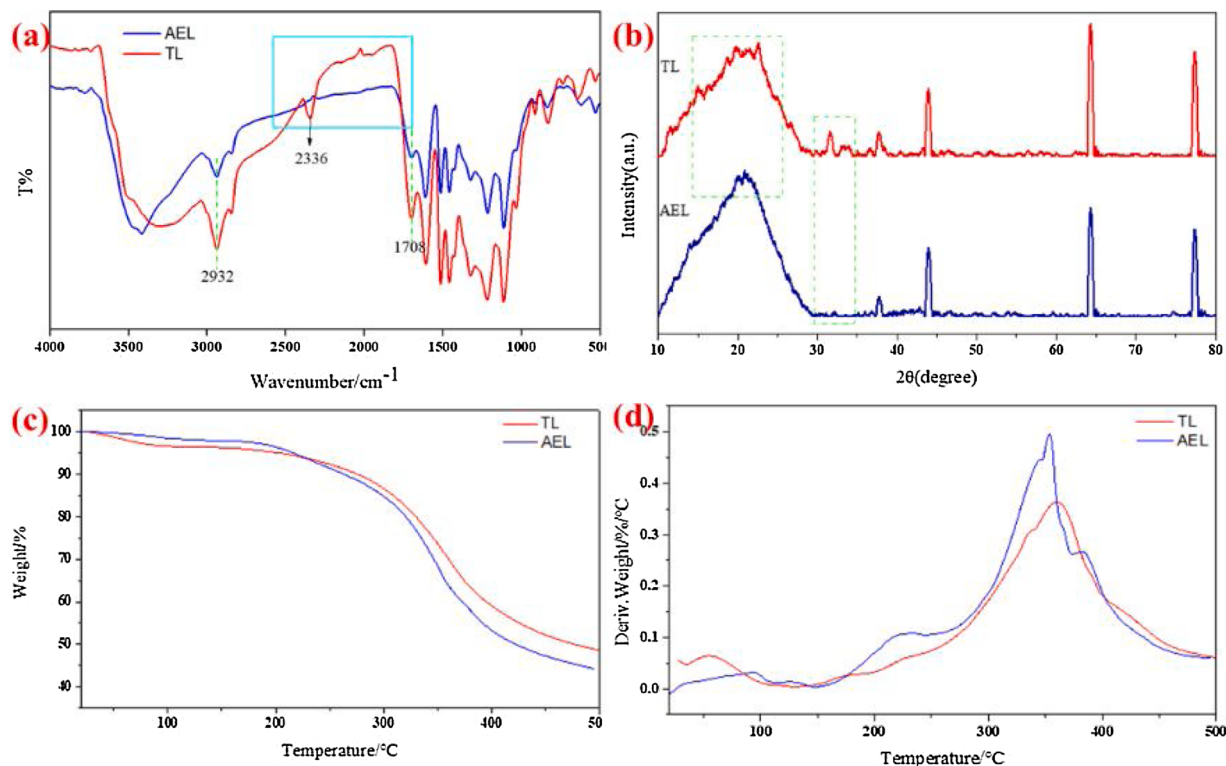


**Fig. 2.** Characterization of TL and AEL: (a) FTIR spectra, (b) XRD patterns, (c) TG curves, (d) DTG curves.

### 2.3. Analytical methods

#### 2.3.1. Characterization

Fourier transform infrared (FTIR) spectra were obtained using a FTIR spectrometer (PE, USA). The water contact angle tests were carried out with an optical contact angle system, and each sample was tested at more than three different locations. X-ray diffraction (XRD) patterns were measured using an X-ray diffractometer ( $(\lambda = 0.1785 \text{ nm})$ ). Thermogravimetric (TG) curves were measured on a simultaneous thermal analyzer (TA Instruments, USA) with a heating rate of  $10 \text{ }^{\circ}\text{C min}^{-1}$  in flowing air. The surface morphology of the filter papers was performed on a JSM-7800 F field emission scanning electron microscope (FESEM) operated (JEOL, Japan). Surface elemental analysis of the filter paper was operated using an energy dispersive X-ray microanalysis system (EDX) attached to the SEM instrument (OXFORD Instruments, Japan).

#### 2.3.2. Resistance to mechanical damage tests

Finger wipe, adhesive tape peeling, knife scratching, and sandpaper abrasion were used in the mechanical damage tests for the as-prepared AEL-FP. In the finger wipe test, a finger was wiped across the surface of AEL-FP repeatedly. The adhesive tape was attached to the surface of AEL-FP, then the adhesive tape was peeled off the paper in the adhesive tape peeling tests. A knife was used to scratch AEL-FP in the knife scratching tests. In the sandpaper abrasion, AEL-FP was abraded using sandpaper. Then, water contact angles of damaged AEL-FP were measured.

#### 2.3.3. Oil/water separation test

The as-prepared AEL-FP was impregnated into oil/water mixtures to remove oil content from the water. The three kinds of oils used in this study were chloroform, petroleum ether and n-hexane. The oil and organic solution were dyed red, and the water was dyed blue for easy distinction.

The filter paper before and after modification was placed in the filter tank and mixed liquid (water, chloroform, petroleum ether, and n-

hexane) was added to measure the amount of liquid passing through the filter paper. The filtration efficiency  $S$  was calculated by weight measurement at room temperature as previously reported (Kong et al., 2014). The density of oil was small and would float on the water surface, so in the experiment, the two components were strictly mixed through a nitrogen bubble to ensure that each phase was fully in contact with the filter paper surface. Once the colored oil was completely filtered out, the separation process was counted as end. The remaining colorless water in the filter tank was named  $m_1$ , the total amount of water added to the filter tank was named  $m_0$  and the separation efficiency  $S$  (%) was calculated as  $S = m_1/m_0$ .

In order to measure the flux, 20 mL of the chloroform-water mixture was poured into the separation device. The separation flux was calculated by recording the time required to separate the 10 mL chloroform. The calculation formula for the separation flux is as follows:

$$\text{Flux} = V/St$$

Where  $V$  (L) is the permeate volume of the emulsion,  $S$  ( $\text{m}^2$ ) is the effective contact area of the modified filter paper, and  $t$  (h) is the separation time.

## 3. Results and discussion

### 3.1. Characterization of the multifunctional AEL-FP

#### 3.1.1. Characterization of TL and AEL

The FT-IR, XRD and TG spectra of TL and AEL were illustrated in Fig. 2. According to the reported literatures (Mohamad Ibrahim et al., 2011), the bands at  $3540 \sim 3700 \text{ cm}^{-1}$  were attributed to the stretching vibration of phenolic hydroxyl groups and the absorption peak at  $2932 \text{ cm}^{-1}$  was related to the stretching vibration of  $-\text{OCH}_3$ . The peaks at  $2336 \text{ cm}^{-1}$  might contribute to the absorption of the cumulative double bonds of TL, which was disappeared on the spectrum of AEL. These lignin samples showed bands at about  $1606 \text{ cm}^{-1}$ ,  $1513 \text{ cm}^{-1}$  and  $1458 \text{ cm}^{-1}$ , which were corresponding to aromatic ring vibrations of the

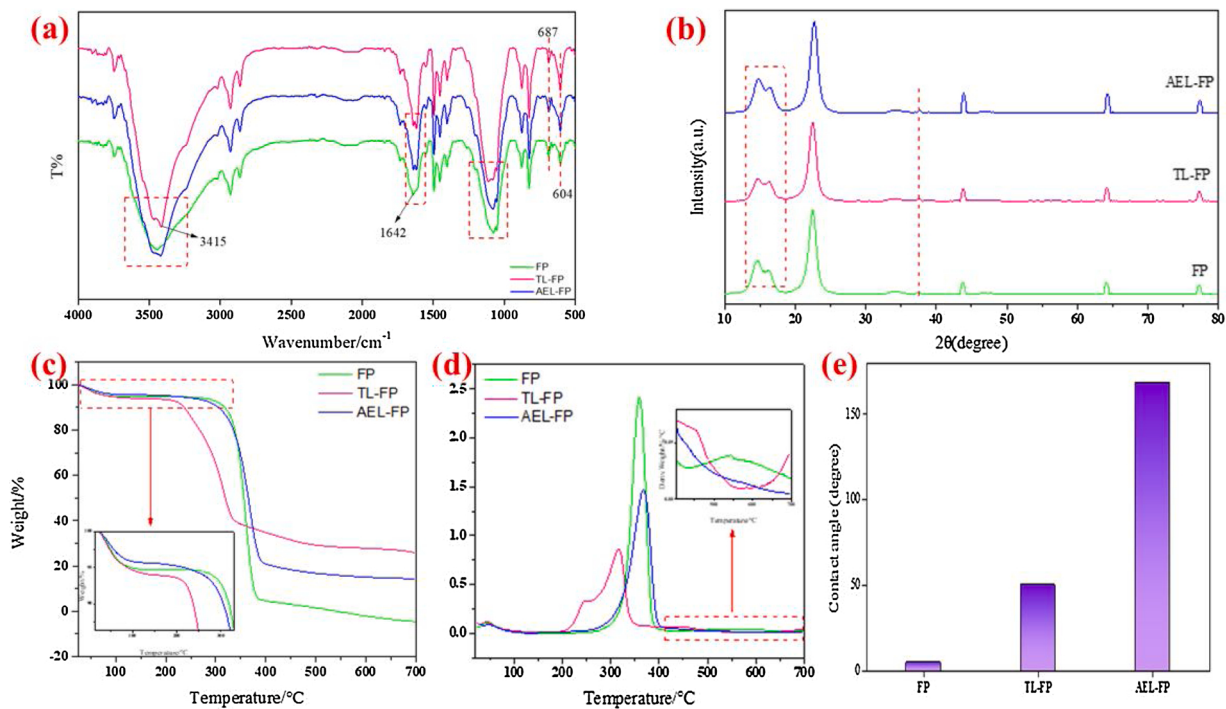


**Fig. 3.** Characterization of FP, TL-FP and AEL-FP: (a) FTIR spectra, (b) XRD patterns, (c) TG curves, (d) DTG curves, (e) water contact angles.

phenyl-propane ( $C_9$ ) skeleton. In Fig. 2a, the absorption peak at  $1708\text{ cm}^{-1}$  of AEL was higher than that of TL, indicating that the extracted lignin had more symmetric ester bond, supporting that AEL was better attached to the filter paper than the TL.

The crystallographic structures of TL and AEL were analyzed by X-ray Diffraction technique. As can be seen in Fig. 2b, the full width at half maximum of AEL was narrower at  $2\theta$  of  $10^\circ\text{--}30^\circ$ , impurities such as metal ions in the  $30^\circ\text{--}35^\circ$  range were also absent in the AEL spectra, indicating that the crystallinity of AEL was higher than that of TL.

Next, the initial decomposition temperature at which maximum decomposition takes place, the weight loss for each thermal stage and the decomposition temperatures and percentage weight loss values of the TL and AEL were shown in Fig. 2c. The initial weight loss in the first

temperature range of  $20\text{ }^\circ\text{C}\text{--}300\text{ }^\circ\text{C}$  was contributed to the evaporation of the residual water and low molecular saccharide. At this stage, 13.3% and 15.12% weight loss were observed for TL and AEL, respectively. At above  $300\text{ }^\circ\text{C}$ , a quick and rapid weight loss was observed in DTG curves (Fig. 2d). TL lost 38.2%, while AEL lost 40.63% weight, in the case a higher weight loss in the second stage was possibly attributed to the breakdown of side chains present on the lignin backbone. Compared with TL it could be seen that the thermal stability of AEL was not significantly reduced, indicating that AEL still keeps a good three-dimensional network structure.

### 3.1.2. Characterization of the FP, TL-FP and AEL-FP

The FT-IR spectra of FP, TL-FP and AEL-FP were illustrated in Fig. 3a, the latter two of which were roughly similar. The intensity of the hydroxyl absorption peak of AEL-FP near  $3410\text{ cm}^{-1}$  was much higher than that of FP. AEL exposed more hydroxyl groups and could form more hydrogen bonds with the bare paper, which facilitate in fixing lignin on the paper surface. At  $1642\text{ cm}^{-1}$ , the absorption peak of FP changed from a sharp peak to two closely connected peaks, and the absorption peaks of AEL-FP at  $1100\text{ cm}^{-1}$ ,  $604\text{ cm}^{-1}$  were narrower and sharper than those of FP.

The crystallographic structures of FP, TL-FP and AEL-FP were examined using X-ray Diffraction technique and shown in Fig. 3b. The three filter papers all had similar peaks at  $2\theta$  range of  $40^\circ\text{--}80^\circ$ , except that the half-width of AEL-FP was slightly narrower at  $2\theta$  range of  $10^\circ\text{--}20^\circ$ , impurities such as metal ions at  $2\theta$  range of  $50^\circ\text{--}60^\circ$  were also absent in the AEL-FP spectra.

The membranes' thermal stability was evaluated by TGA, as shown in Fig. 3c and d. The TGA curves of FP, TL-FP and AEL-FP were divided into three main regions: the first one from  $20\text{ }^\circ\text{C}$  to  $300\text{ }^\circ\text{C}$ , the second one from  $300\text{ }^\circ\text{C}$  to  $400\text{ }^\circ\text{C}$  and the third one from  $400\text{ }^\circ\text{C}$  to  $700\text{ }^\circ\text{C}$ . The initial weight loss in the first temperature region of  $20\text{ }^\circ\text{C}\text{--}300\text{ }^\circ\text{C}$  was contributed to the evaporation of water and low molecular saccharide. At this stage, 7.02%, 34.88% and 9.12% weight loss were observed for FP, TL-FP and AEL-FP, respectively. As temperature increasing to above  $300\text{ }^\circ\text{C}$ , a quick and rapid weight loss was observed in DTG curves (Fig. 3d). After thermal degradation at  $400\text{ }^\circ\text{C}$ , the percentages of the

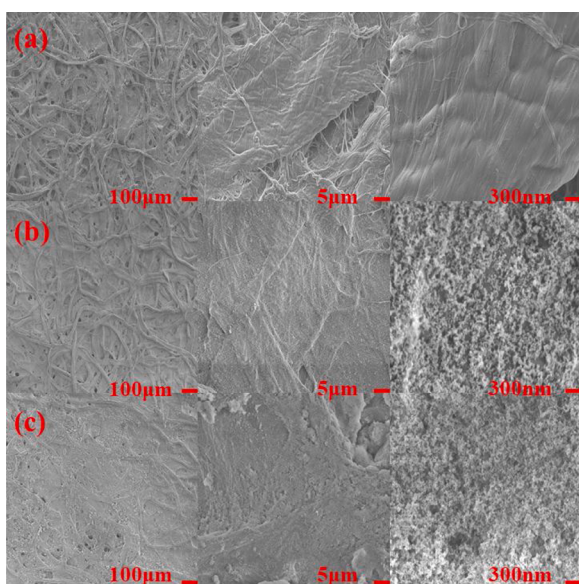


**Fig. 4.** SEM images of the filter paper before and after modification: (a)FP; (b)TL-FP; (c) AEL-FP.

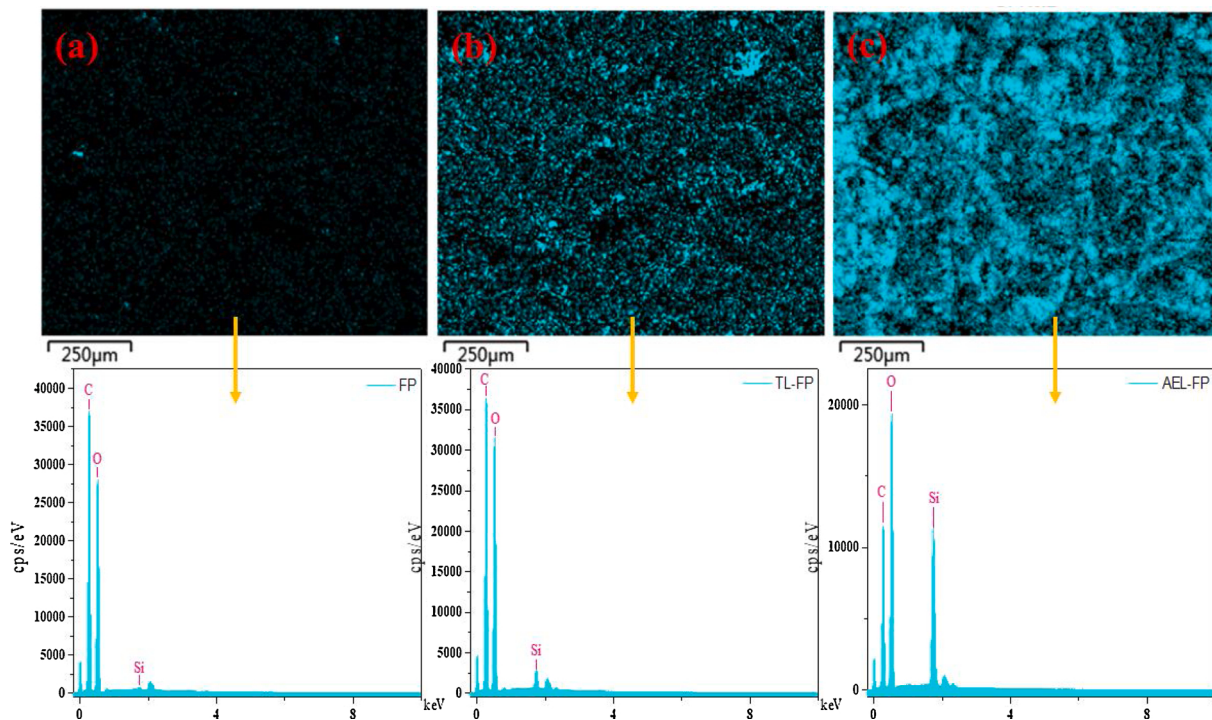


Fig. 5. EDS analysis of the filter paper before and after modification: (a)FP; (b) TL-FP; (c) AEL-FP.

weight loss for FP, TL-FP and AEL-FP were 88.18%, 30.32% and 70.02% respectively.

The water contact angles were carried out to characterize the surface wettability of the as-prepared filter paper. As shown in Fig. 3e, the water contact angles of the FP, TL—FP and AEL-FP were measured to be 0°, 50°, and 168°, respectively, revealing the superhydrophobic properties of AEL-FP surface and the hydrophilic property of FP and TL—FP surface. This situation might be due to that FP had formed a more stable hydrogen bond network on the surface after lignin immersion. At the same time, AEL had exposed more hydroxyl, carboxyl groups and more symmetric ester bond after acetonitrile extraction, which was better attached to the filter paper and had a better retention effect on silica nanoparticles to form hydrophobic micro-nano binary structure that leads to a big water contact angle.

### 3.1.3. SEM-EDS analysis

The microstructure and roughness of the material surface could play an important role in its wettability. The SEM images of the FP, TL-FP and AEL-FP were shown in Fig. 4. The untreated filter paper was a three-dimensional network structure consisting of a large number of interwoven plant fibers. In the zoom-in view, the surface of the single fiber was smooth. Fig. 4b and c were the micromorphology of TL-FP and AEL-FP. It was obvious that the surface of the single fiber became coarse, and the voids between the original fibers were filled by lignin and SiO<sub>2</sub> nanoparticles. The SiO<sub>2</sub> nanoparticles were more evenly distributed on the lignin microparticles, creating a stable and hydrophobic micro-nano binary structure for oil-water separation.

Furthermore, with the aim of understanding the surface elemental distribution, the FP, TL—FP and AEL-FP were analyzed by EDS (Fig. 5).

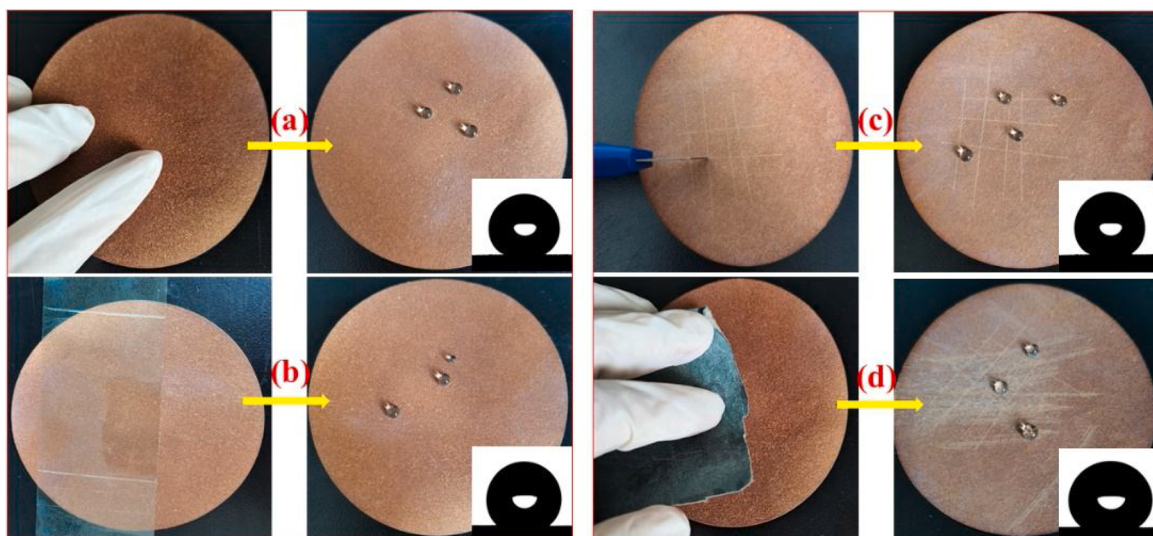
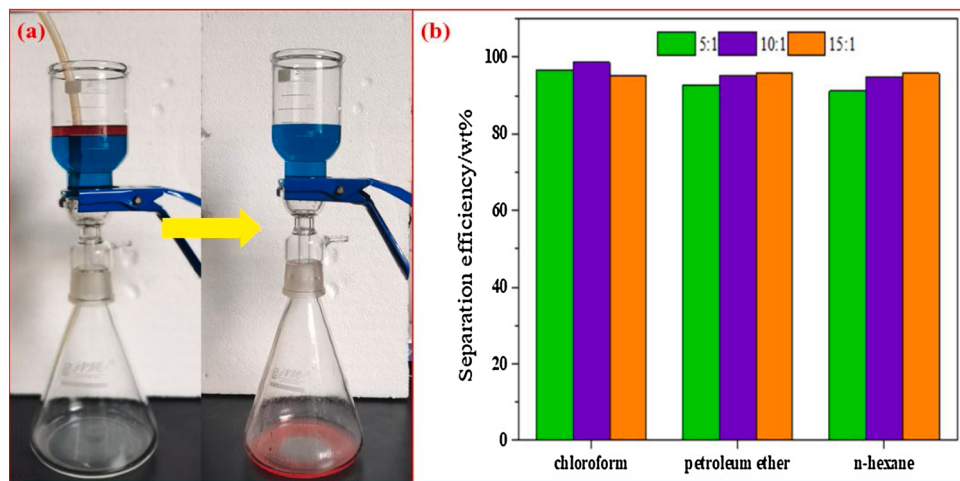
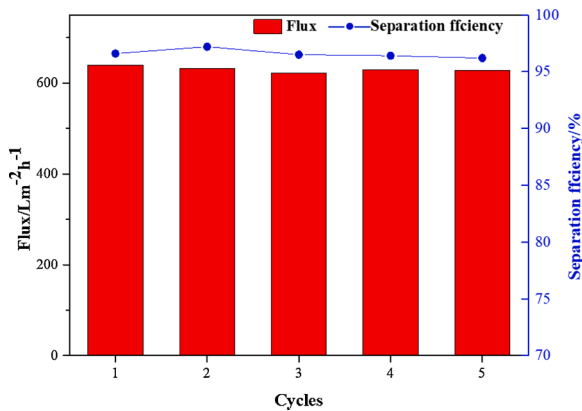


Fig. 6. Digital images of water droplets of the paper after different physical damages: (a) finger wipe, (b) adhesive tape peeling, (c) knife scratching, (d) sandpaper abrasion.



**Fig. 7.** Separation efficiencies of the modified filter papers for different oil/water mixture systems (water: oil mass ratio = 5:1, 10:1, 15:1).



**Fig. 8.** Oil permeation flux and oil/water separation efficiency by using AEL-PF in different cycles.

The silicon content of FP was only 0.22%, and that of TL—FP was 1.44% and nano-silica retention rate was too low (Fig. 5b). On the other hand, it could be seen in Fig. 5c that the distribution of silicon on AEL-FP had reached 11.57%, and it was denser and more uniform. This is attributed to the more exposed hydroxyl and carboxyl groups on AEL after acetonitrile extraction, which is advantageous for forming hydrogen bonds with the nano silica, thus benefit in retaining more nano silica particles on AEL-FP and forming a superhydrophobic surface for oil-water separation.

### 3.2. Super-hydrophobic stability of the AEL-FP

The stability of superhydrophobic materials was important for practical applications (Yang et al., 2018). The mechanical damage might decrease the superhydrophobic function. In this research work, several mechanical damage tests, including finger wipe, adhesive tape peeling, knife scratching and sandpaper abrasion, were performed to evaluate the stability of AEL-FP. As shown in Fig. 6, AEL-FP was able to well preserve its super-hydrophobicity after different mechanical damages. The water droplets on the surface of the damaged paper were still nearly spherical, and the corresponding contact angles were all above 155°, indicating that the superhydrophobic AEL-FP had a high mechanical durability.

### 3.3. Oil/water separation performance

The oil-water separation performance of the modified filter paper

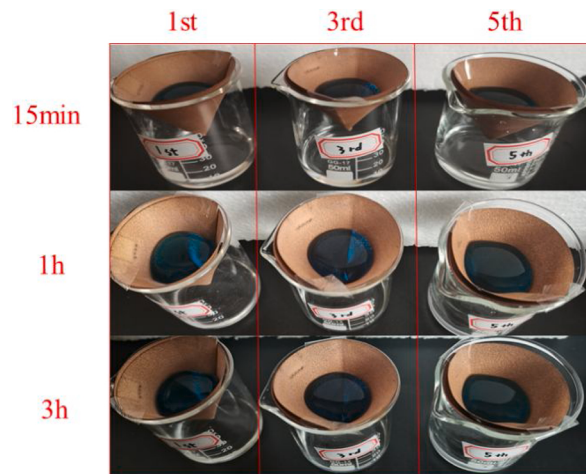


**Fig. 9.** Separation images of oil/water mixture under different separation period (15 min, 1 h and 3 h after oil completed permeated through the filter paper) in recycle test.

was tested based on the ratio of the remaining water in the filter to the initial feed water when separating the different oil/water mixtures, and the processes before and after the separation were shown in Fig. 7a. Fig. 7b showed that the separation efficiencies for three kinds of oil (chloroform, petroleum ether and n-hexane) are all higher than 90% (up to 98.6% for chloroform), revealing the good applicability for various oil samples.

To evaluate the recyclability, the AEL-PF is repeatedly used for the oil/water separation. The oil flux and separation efficiency to chloroform for five cycles are showed in Fig. 8, and it is found that the efficiency is kept at 96.6% during all the cyclic tests, indicating a good recyclability of the AEL-PF. The pristine filter paper before surface modification demonstrates a high oil flux of  $655.4 \text{ L} \cdot \text{m}^{-2} \cdot \text{h}^{-1}$ , which slight decreased to around  $635.6 \text{ L} \cdot \text{m}^{-2} \cdot \text{h}^{-1}$  after 5 cycles, which demonstrated the superhydrophobic filter paper is no discernible effect on the flux.

### 3.4. Durability test

Considering that the filter paper is easily damaged, the durability was tested. The results showed that the modified paper have a good durability. Oil/water separation states under different period and recycling times were shown in Fig. 9. All samples in Fig. 9 achieved

complete oil/water separation within 15 min, although after five repeatable separation cycles, the modified paper filter for oil/water mixture separation kept no damage even after 3 h, just a slight residue.

#### 4. Conclusion

A highly efficient and low-cost membrane based on filter paper, lignin and silica was developed in this work. The preparation of the membrane is a very simple process consisting of two-step impregnation in which a thin layer of lignin is firstly coated on the surface of the filter paper, and then the silica nanoparticles are adhered to the pre-coated lignin layer. The surface modification successfully transforms the hydrophilic nature of the filter papers to hydrophobic and oleophilic. More importantly, this simple modification method is expected to easily convert the surface properties of a variety of substrates from hydrophilic into hydrophobic. The as-prepared AEL-FP revealing excellent separation efficiency for oil/water separation, reaching separation efficiency up to 98.6%, indicating it great potential in the application of many fields, such as oil collection device, continuous oil-water separation, oily wastewater treatment, and environmental protection.

#### CRediT authorship contribution statement

**Xiaoyu Gong:** Investigation, Writing - original draft. **Yi Meng:** Conceptualization, Writing - review & editing. **Junjie Zhu:** Investigation. **Xing Wang:** Software. **Jie Lu:** Supervision. **Yi Cheng:** Software, Supervision. **Yehan Tao:** Supervision, Writing - review & editing. **Hai-song Wang:** Project administration, Supervision, Writing - review & editing.

#### Declaration of Competing Interest

We declare that we have no financial and personal relationships with other people or organizations that can inappropriately influence our work, there is no professional or other personal interest of any nature or kind in any product, service and/or company that could be construed as influencing the position presented in, or the review of, the manuscript entitled, “Construct a stable super-hydrophobic surface through acetonitrile extracting lignin and nano-silica and its application in oil-water separation”.

#### Acknowledgments

The authors are grateful for the National Key R&D Program of China (No. 2018YFD0400703), the financial support from the Natural Science Foundation of China (No. 31770624 and No.21978029) and Liaoning BaiQianWan Talents Program (201945).

#### Appendix A. Supplementary data

Supplementary material related to this article can be found, in the online version, at doi:<https://doi.org/10.1016/j.indcrop.2021.113471>.

#### References

- Chen, S., Song, Y., Xu, F., 2018. Highly transparent and hazy cellulose nanopaper simultaneously with a self-cleaning superhydrophobic surface. *ACS Sustain. Chem. Eng.* 6, 5173–5181.
- Chen, S., Zhou, Y., Liu, H., Yang, J., Wei, Y., Zhang, J., 2019. Synthesis and physicochemical investigation of anionic-nonionic surfactants based on lignin for application in enhanced oil recovery. *Energy Fuels* 33, 6247–6257.
- Cheryan, M., Rajagopalan, N., 1998. Membrane processing of oily streams. *Wastewater treatment and waste reduction*. *J. Memb. Sci.* 151, 16.
- Chio, C., Sain, M., Qin, W., 2019. Lignin utilization: a review of lignin depolymerization from various aspects. *Renewable Sustainable Energy Rev.* 107, 232–249.
- Cui, M., Nguyen, N.A., Bonnesen, P.V., Uhrig, D., Keum, J.K., Naskar, A.K., 2018. Rigid oligomer from lignin in designing of tough, self-healing elastomers. *ACS Macro Lett.* 7, 1328–1332.
- Feng, L., Zhang, Z., Mai, Z., Ma, Y., Liu, B., Jiang, L., Zhu, D., 2004. A super-hydrophobic and super-oleophobic coating mesh film for the separation of oil and water. *Angew. Chemie* 116, 2046–2048.
- Fu, S., Zhou, H., Wang, H., Niu, H., Yang, W., Shao, H., Wang, J., Lin, T., 2019. Superhydrophilic, underwater directional oil-transport fabrics with a novel oil trapping function. *ACS Appl. Mater. Interfaces* 11, 27402–27409.
- Gong, X., Liu, T., Yu, S., Meng, Y., Lu, J., Cheng, Y., Wang, H., 2020. The preparation and performance of a novel lignin-based adhesive without formaldehyde. *Ind. Crops Prod.* 153.
- Hu, Z., Zen, X., Gong, J., Deng, Y., 2009. Water resistance improvement of paper by superhydrophobic modification with microsized  $\text{CaCO}_3$  and fatty acid coating. *Colloids Surf. A Physicochem. Eng. Asp.* 351, 65–70.
- Kłapiszewski, L., Szalaty, T.J., Gras, M., Moszynski, D., Buchwald, T., Lota, G., Jesionowski, T., 2020. Lignin-based dual component additives as effective electrode material for energy management systems. *Int. J. Biol. Macromol.* 165, 268–278.
- Kong, L., Wang, Q., Xiong, S., Wang, Y., 2014. Turning low-cost filter papers to highly efficient membranes for oil/water separation by atomic-layer-deposition-enabled hydrophobization. *Ind. Eng. Chem. Res.* 53, 16516–16522.
- Li, M., Xu, J., Lu, Q., 2007. Creating superhydrophobic surfaces with flowery structures on nickel substrates through a wet-chemical-process. *J. Mater. Chem.* 17.
- Liu, Y., Liu, J., Li, S., Liu, J., Han, Z., Ren, L., 2013. Biomimetic superhydrophobic surface of high adhesion fabricated with micronano binary structure on aluminum alloy. *ACS Appl. Mater. Interfaces* 5, 8907–8914.
- Lu, J., Liu, H., Xia, F., Zhang, Z., Huang, X., Cheng, Y., Wang, H., 2020. The hydrothermal-alkaline/oxygen two-step pretreatment combined with the addition of surfactants reduced the amount of cellulase for enzymatic hydrolysis of reed. *Bioresour. Technol.* 308, 123324.
- Ma, M., Hill, R.M., Lowery, J.L., Fridrikh, S.V., Rutledge, G.C., 2005. Electrospun poly (Styrene-block-dimethylsiloxane) block copolymer fibers exhibiting superhydrophobicity. *Langmuir* 21.
- Meng, Y., Liu, T., Yu, S., Cheng, Y., Lu, J., Wang, H., 2020. A lignin-based carbon aerogel enhanced by graphene oxide and application in oil/water separation. *Fuel* 278, 118376.
- Mohamad Ibrahim, M.N., Zakaria, N., Sipaut, C.S., Sulaiman, O., Hashim, R., 2011. Chemical and thermal properties of lignins from oil palm biomass as a substitute for phenol in a phenol-formaldehyde resin production. *Carbohydr. Polym.* 86, 112–119.
- Peng, R., Pang, Y., Qiu, X., Qian, Y., Zhou, M., 2020. Synthesis of anti-photolysis lignin-based dispersants and its application in pesticide suspension concentrate. *RSC Adv.* 10, 13830–13837.
- Raj, A., Devendra, L.P., Sukumaran, R.K., 2020. Comparative evaluation of laccase mediated oxidized and unoxidized lignin of sugarcane bagasse for the synthesis of lignin-based formaldehyde resin. *Ind. Crops Prod.* 150.
- Roy, D., Semsarilar, M., Guthrie, J.T., Perrier, S., 2009. Cellulose modification by polymer grafting: a review. *Chem. Soc. Rev.* 38, 2046–2064.
- Shamaei, L., Khorshidi, B., Islam, M., Sadrzadeh, M., 2020. Industrial waste lignin as an antifouling coating for the treatment of oily wastewater: creating wealth from waste. *J. Clean. Prod.* 256, 120304.
- Tang, X., Shen, C., Zhu, W., Zhang, S., Xu, Y., Yang, Y., Gao, M., Dong, Fu., 2017. A facile procedure to modify filter paper for oil–water separation. *RSC Adv.* 7 (48), 30495–30499.
- Venkatesagowda, B., Dekker, R.F.H., 2019. Enzymatic demethylation of Kraft lignin for lignin-based phenol-formaldehyde resin applications. *Biomass Convers. Biorefinery* 10, 203–225.
- Wang, S., Li, M., Lu, Q., 2010. Filter paper with selective absorption and separation of liquids that differ in surface tension. *ACS Appl. Mater. Interfaces* 2, 677–683.
- Wang, Y.T., He, B.H., Zhao, L.H., 2017. Fabrication of hydrophobic coating on filter paper from self-emulsifying carnauba wax-alcohol emulsions with nano-TiO<sub>2</sub> particles for water/diesel separation. *Bioresources* 12 (4), 7774–7783.
- Wen, J.L., Sun, S.L., Xue, B.L., Sun, R.C., 2013. Recent advances in characterization of lignin polymer by solution-state nuclear magnetic resonance (NMR) methodology. *Materials* 6, 359–391.
- Xia, F., Gong, J., Lu, J., Cheng, Y., Zhai, S., An, Q., Wang, H., 2020. Combined liquid hot water with sodium carbonate-oxygen pretreatment to improve enzymatic saccharification of reed. *Bioresour. Technol.* 297, 122498.
- Xu, X., Zhang, Z., Guo, F., Yang, J., Zhu, X., 2011. Fabrication of superhydrophobic binary nanoparticles/PMMA composite coating with reversible switching of adhesion and anticorrosive property. *Appl. Surf. Sci.* 257, 7054–7060.
- Yan, S., Li, Y., Xie, F., Wu, J., Jia, X., Yang, J., Song, H., Zhang, Z., 2020. Environmentally safe and porous MS@TiO<sub>2</sub>@PPy monoliths with superior visible-light photocatalytic properties for rapid oil-water separation and water purification. *ACS Sustain. Chem. Eng.* 8, 5347–5359.
- Yang, R.-L., Zhu, Y.-J., Chen, F.-F., Qin, D.-D., Xiong, Z.-C., 2018. Recyclable, fire-resistant, superhydrophobic, and magnetic paper based on ultralong hydroxyapatite nanowires for continuous oil/water separation and oil collection. *ACS Sustain. Chem. Eng.* 6, 10140–10150.
- Zhang, Y., Zhang, Y., Cao, Q., Wang, C., Yang, C., Li, Y., Zhou, J., 2019. Novel porous oil-water separation material with super-hydrophobicity and super-oleophilicity prepared from beeswax, lignin, and cotton. *Sci. Total Environ.* 706, 135807.
- Zhang, S., Huang, X., Wang, D., Xiao, W., Huo, L., Zhao, M., Wang, L., Gao, J., 2020. Flexible and superhydrophobic composites with dual polymer nanofiber and carbon nanofiber network for high-performance chemical vapor sensing and Oil/Water separation. *ACS Appl. Mater. Interfaces* 12, 47076–47089.
- Zhu, Q., Pan, Q., Liu, F., 2011. Facile removal and collection of oils from water surfaces through superhydrophobic and superoleophilic sponges. *J. Phys. Chem. C* 115, 17464–17470.